



Characterization of Highly Sulfonated SIBS Polymer Partially Neutralized With Mg^{+2} Cations

by Eugene Napadensky and James M. Sloan

ARL-TR-4528

August 2008

NOTICES

Disclaimers

The findings in this report are not to be construed as an official Department of the Army position unless so designated by other authorized documents.

Citation of manufacturer's or trade names does not constitute an official endorsement or approval of the use thereof.

Destroy this report when it is no longer needed. Do not return it to the originator.

Army Research Laboratory

Aberdeen Proving Ground, MD 21005-5069

ARL-TR-4528**August 2008**

Characterization of Highly Sulfonated SIBS Polymer Partially Neutralized With Mg^{+2} Cations

Eugene Napadensky and James M. Sloan
Weapons and Materials Research Directorate, ARL

| REPORT DOCUMENTATION PAGE | | | | Form Approved OMB No. 0704-0188 | |
|--|-----------------------------|------------------------------|---|--|---|
| Public reporting burden for this collection of information is estimated to average 1 hour per response, including the time for reviewing instructions, searching existing data sources, gathering and maintaining the data needed, and completing and reviewing the collection information. Send comments regarding this burden estimate or any other aspect of this collection of information, including suggestions for reducing the burden, to Department of Defense, Washington Headquarters Services, Directorate for Information Operations and Reports (0704-0188), 1215 Jefferson Davis Highway, Suite 1204, Arlington, VA 22202-4302. Respondents should be aware that notwithstanding any other provision of law, no person shall be subject to any penalty for failing to comply with a collection of information if it does not display a currently valid OMB control number. PLEASE DO NOT RETURN YOUR FORM TO THE ABOVE ADDRESS. | | | | | |
| 1. REPORT DATE (DD-MM-YYYY) August 2008 | | 2. REPORT TYPE Final | | 3. DATES COVERED (From - To) October 2006–October 2007 | |
| 4. TITLE AND SUBTITLE Characterization of Highly Sulfonated SIBS Polymer Partially Neutralized With Mg ⁺² Cations | | | | 5a. CONTRACT NUMBER | |
| | | | | 5b. GRANT NUMBER | |
| | | | | 5c. PROGRAM ELEMENT NUMBER | |
| 6. AUTHOR(S) Eugene Napadensky and James M. Sloan | | | | 5d. PROJECT NUMBER AH84 | |
| | | | | 5e. TASK NUMBER | |
| | | | | 5f. WORK UNIT NUMBER | |
| 7. PERFORMING ORGANIZATION NAME(S) AND ADDRESS(ES) U.S. Army Research Laboratory ATTN: AMSRD-ARL-WM-MA Aberdeen Proving Ground, MD 21005-5069 | | | | 8. PERFORMING ORGANIZATION REPORT NUMBER ARL-TR-4528 | |
| 9. SPONSORING/MONITORING AGENCY NAME(S) AND ADDRESS(ES) | | | | 10. SPONSOR/MONITOR'S ACRONYM(S) | |
| | | | | 11. SPONSOR/MONITOR'S REPORT NUMBER(S) | |
| 12. DISTRIBUTION/AVAILABILITY STATEMENT Approved for public release; distribution is unlimited. | | | | | |
| 13. SUPPLEMENTARY NOTES | | | | | |
| 14. ABSTRACT <p>In the search for selective membranes capable of separating protons from methanol for direct methanol fuel cells or chemical and biological toxins from water in chemical protective clothing, block copolymer ionomer membranes emerge. They are highly ordered sequence of both ionic and nonionic blocks, in which the ionic groups are randomly arranged along the polymer chain. This investigation studied one of these block copolymer ionomers, sulfonated poly(styrene-b-isobutylene-b-styrene).</p> <p>In this study, the characterization of transport properties and chemical structure of sulfonated poly(styrene-b-isobutylene-b-styrene) block copolymers that are partially crosslinked to a various levels with magnesium ions are reported. The vapor transport and solubility properties of both water and dimethyl-methyl phosphonate (DMMP) were studied as a function of concentration of magnesium ion exchanged into the sulfonated domains of the SIBS ionomer. The results indicate that vapor transport of both water and DMMP are significantly decreased when Mg⁺² is incorporated into the ionic polymer. Fourier-transform infrared spectroscopy results revealed that a significant amount of ordering occurred as a result on the incorporation of Mg⁺² ions. All the Mg⁺² ions were localized into the sulfonated domains, resulting in a tighter molecular packing arrangement and thus a more ordered structure. It is this ordered structure that causes the improvement in the transport properties.</p> | | | | | |
| 15. SUBJECT TERMS ionomers, chem-bio, breathability, membrane, FTIR, TGA, vapor transport | | | | | |
| 16. SECURITY CLASSIFICATION OF: | | | 17. LIMITATION OF ABSTRACT UL | 18. NUMBER OF PAGES 30 | 19a. NAME OF RESPONSIBLE PERSON Eugene Napadensky |
| a. REPORT UNCLASSIFIED | b. ABSTRACT UNCLASSIFIED | c. THIS PAGE UNCLASSIFIED | | | 19b. TELEPHONE NUMBER (Include area code) 410-306-0682 |

Contents

| | |
|--|-----------|
| List of Figures | iv |
| List of Tables | iv |
| 1. Introduction | 1 |
| 2. Experimental | 2 |
| 2.1 Materials | 2 |
| 2.2 Membrane Preparation | 2 |
| 3. Characterization | 3 |
| 3.1 Fourier-Transform Infrared Spectroscopy (FTIR) | 3 |
| 3.2 Elemental Analysis | 3 |
| 3.3 Solubility | 4 |
| 3.4 Vapor Transport Measurements | 4 |
| 3.5 Thermogravametric Analysis | 5 |
| 4. Results and Discussion | 5 |
| 4.1 Levels of Mg Exchange | 5 |
| 4.2 FTIR | 6 |
| 4.3 Solubility | 9 |
| 4.4 Vapor Transport Rate | 9 |
| 4.5 TGA | 12 |
| 5. Conclusions | 14 |
| 6. References | 16 |
| Appendix A. Solubility and Transport Data | 19 |
| Appendix B. TGA Data | 21 |
| Distribution List | 23 |

List of Figures

| | |
|--|----|
| Figure 1. Sulfonation reaction scheme..... | 2 |
| Figure 2. Modification of sulfonated SIBS with Mg^{+2} ions..... | 3 |
| Figure 3. Schematic showing cutaways of the vial-cap and the cap-membrane assemblies used for VTR data collection. | 4 |
| Figure 4. Efficiency of Mg^{+2} - SO_3 complexation reaction..... | 6 |
| Figure 5. FTIR comparison of sulfonated (S-97-SIBS) and unsulfonated SIBS membranes. Asterisks mark the IR bands associated with sulfonate groups. | 7 |
| Figure 6. FTIR spectra for neutralized and partially neutralized and non-neutralized SIBS-Mg ionomer, (a) Mg-SIBS-0, (b) Mg-SIBS-25, (c) Mg-SIBS-50, (d) Mg-SIBS-75, (e) Mg-SIBS-100, and (f) Mg-SIBS-Max..... | 8 |
| Figure 7. Normalized IR intensity of the 1168 cm^{-1} absorption band with increasing Mg content. This band indicates Mg complexation formed when two or more sulfonate groups ionically bonded to the Mg^{+2} cation..... | 8 |
| Figure 8. Correlation between water sorption and Mg exchange level. | 9 |
| Figure 9. Effect of Mg^{+2} loading on water and DMMP vapor transport. | 10 |
| Figure 10. Water-DMMP selectivity of Mg^{+2} exchanged SIBS. | 11 |
| Figure 11. Correlation between water and DMMP vapor transport rates..... | 12 |
| Figure 12. Visual representation of shift in SO_3 decomposition temperature, (a) as an overlay of DTGA curves and (b) as a plot of the onset temperature vs. % Mg^{+2} exchange levels. | 13 |
| Figure 13. Increase in area under SO_3 -Mg complex decomposition curves, (a) as an overlay of DTGA curves and (b) as a plot of the area vs. % Mg^{+2} exchange levels. | 15 |

List of Tables

| | |
|--|----|
| Table 1. Ion exchange levels and elemental analysis results. | 5 |
| Table 2. Estimated magnesium levels for low exchange level samples. | 6 |
| Table A-1. Water sorption data..... | 20 |
| Table A-2. Vapor transport data. | 20 |
| Table B-1. TGA data..... | 22 |

1. Introduction

Chemical/biological protective clothing technology remains a high priority among people responsible for the safety of U.S. military personnel. Not just from the obvious point of exposure to chemical or biological agents abroad and at home, but also from another, less often considered, but still important safety factor: breathability. Until recently, the main goal in the development of chemical/biological protective clothing was to maximize protection. In the past, one of the more commonly used materials for this application was butyl rubber working on principle of total blockage. Butyl rubber is an effective barrier to most harmful agents at certain thicknesses, but it has certain disadvantages. Wearing garments manufactured from this material in combat or in other situations which involves physical activity is not practical, since the lack of breathability of this material causes heat fatigue and exhaustion (1). Another approach for protection against chemical/biological threats is sorptive materials. Protective suits such as Military Oriented Protective Posture (MOPP) suit and Joint Service Lightweight Integrated Suit Technology (JSLIST) work on principle of capturing toxic materials with fillers like activated carbon. The JSLIST suit is more breathable, however it does not provide as much protection as butyl rubber, while still remaining heavy and bulky. Working in the suit is limited to about 45 min of each hour (2).

A completely different approach to the problem of chemical/biological protection is the concept of semi-permeable membranes. These materials would allow passage of moisture (perspiration), but block harmful molecules and organisms. Garments utilizing this technology will offer protection in the hostile environment without causing significant heat fatigue and exhaustion. A number of such semi-permeable membranes are being developed in industry and at the U.S. Army Research Laboratory (ARL) (3).

Investigators at ARL have developed a new material, an ionic block copolymer, highly sulfonated poly(styrene-*b*-isobutylene-*b*-styrene) (S-SIBS) (4), which possess many of the desired properties for chem-bio protective clothing. The major component of the triblock copolymer is polyisobutylene (PIB), which comprises 70% by weight of the base polymer. The PIB gives the material low-temperature flexibility as well as excellent barrier properties. The polystyrene (PS) makes up 30% by weight of the material and forms a glassy region which imparts mechanical strength to the polymer film. In the solid state, the thermodynamic immiscibility of the two components results in a microphase separation where domains of PS are formed in the rubbery PIB matrix (5, 6). The fraction of PS controls the resultant morphology, which can be, for example, cylinders, lamellae, spheres, or a complex mixture. Polystyrene blocks of the polymer can be sulfonated to various degrees, creating interconnected hydrophilic pathways within polystyrene regions (7). These pathways allow diffusion of water and other polar molecules through the material. Subsequent modification of the sulfonated domains with

alkaline earth metal ions improves barrier properties required for U.S. Army application (8–10); however, to date, little research has been performed to evaluate effect of partial ion exchange on permeation properties.

2. Experimental

2.1 Materials

Poly(styrene-*b*-isobutylene-*b*-styrene) block copolymer was provided by Kuraray Co., Ltd., Tsukuba research laboratories, with the reported properties: 30.84 weight-percent styrene, 0.95 specific gravity, $M_w = 71,920$ g/mol, $M_n = 48,850$ g/mol, and polydispersity index (PDI) = 1.47. The base material was sulfonated (figure 1) at ARL with acetyl sulfate to 97%. That is 97% of all styrene groups in the polymer were modified with sulfonic acid group as was verified by titration and elemental analysis. The sulfonation procedure is described in detail elsewhere (4). Other materials in this study included: magnesium perchlorate (Acros Organics), water (J.T. Baker, HPLC grade), dimethylmethylphosphonate (Lancaster Synthesis, 97%), Drierite* (Anhydrous Calcium Sulfate, 97%, W.A. Hammond Drierite Co.), acetone (Warner-Graham Co., reagent grade), toluene (EM Science, 99.5%), and hexanol (J.T. Baker).

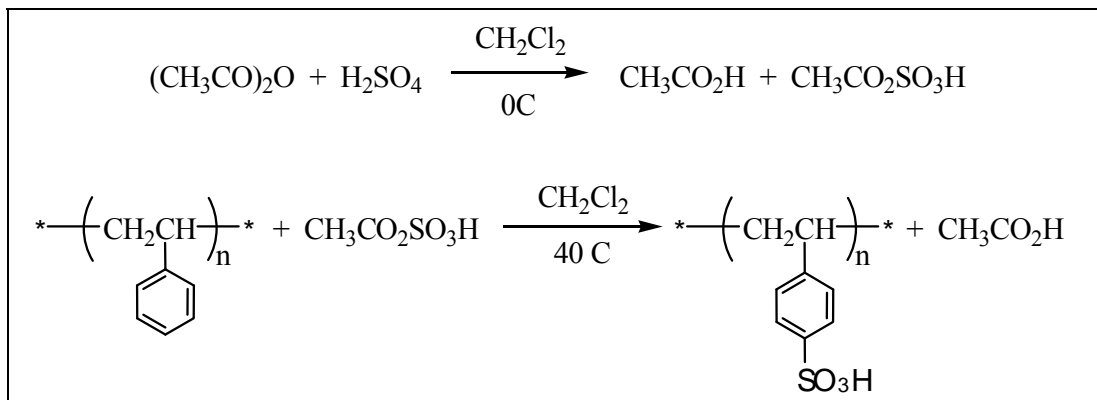


Figure 1. Sulfonation reaction scheme.

2.2 Membrane Preparation

Solution cast membranes were prepared by dissolving 97% sulfonated poly(styrene-*b*-isobutylene-*b*-styrene) (S-97-SIBS) in a mixed solvent of toluene/hexanol (85/15, w/w) at concentration of 2.5% (w/v) and solution casting in open Teflon[†] petri dishes for ~1 week at ambient conditions. The resultant membranes were then further dried/annealed in a vacuum oven at 50 °C for an additional 2 weeks to remove any residual hexanol. This resulted in flexible, 100-μm membrane.

*Drierite is a registered trademark of W.A. Hammond Drierite Co., Xenia, OH.

[†]Teflon is a registered trademark of E.I. DuPont de Nemours and Company, Newark, DE.

Exchange of the acidic hydrogen with Mg^{+2} ions was accomplished by immersing membranes into an aqueous solution of magnesium perchlorate. Under these conditions, the acidic hydrogens are exchanged out with Mg^{+2} ions creating an ionic crosslink between the neighboring sulfonic groups. Initially, attempts were made to control amount of substitution by the varying exposure time that the membranes were in contact with the solution. Due to the speed of the exchange reaction, this method did not result in desired level of control, and an alternative method has to be selected. It was decided that the membranes will be exchanged by immersing them into a magnesium perchlorate solution containing various stoichiometric amounts of magnesium ions. Solution concentrations were varied from 0.004 to 1 equivalent of magnesium salt, taking 1 equivalent as 1:2 molar ratio of Mg^{+2} to SO_3H group. It is assumed that each magnesium ion will be ionically attracted to two sulfuric acid groups, as shown in the figure 2, in order to satisfy the requirements for complete the electron shell of the cation. Subsequently, the samples were numbered reflecting maximum theoretical level of ion exchange. In addition, one membrane was exchanged in solution containing 50 equivalents (5000%) of $\text{Mg}(\text{ClO}_4)_2$, creating membrane with maximum magnesium ions exchange level possible under this experimental conditions.

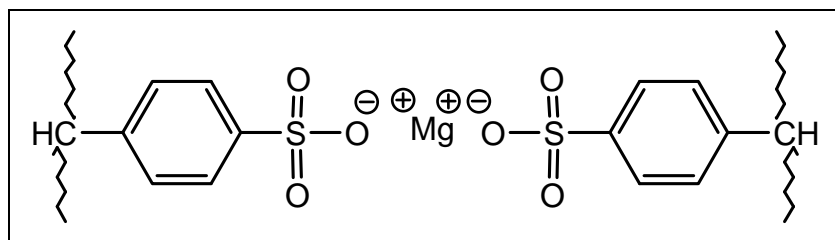


Figure 2. Modification of sulfonated SIBS with Mg^{+2} ions.

3. Characterization

3.1 Fourier-Transform Infrared Spectroscopy (FTIR)

Infrared spectra of all polymer samples were collected using a FTIR spectrometer (Nicolet Magna 560 Series) equipped with a Thunderdome (Spectra-Tech) accessory with a multiple-reflection ATR crystal (ZnSe, refractive index = 2.4). This accessory contains a pressure mechanism for good sample-to-crystal contact. All infrared spectra were collected using 128 scans and 4 cm^{-1} resolution.

3.2 Elemental Analysis

Elemental analysis was performed by Atlantic Microlab, Inc. and Galbraith Laboratories, Inc. This was done to obtain accurate sulfonation levels of the functionalized S-SIBS as well as to determine amount of magnesium present in the membranes. Samples were analyzed for weight percent of carbon, hydrogen, oxygen, sulfur, and magnesium.

3.3 Solubility

Samples were dried in a vacuum oven at 45 °C for 1.5 hr, weighed, and placed into a vial with deionized water for period of 48 hr. At the end of that time samples were removed, excess water was dabbed from the surface and swollen weight was recorded.

3.4 Vapor Transport Measurements

Vapor permeation experiments were conducted based on the modified ASTM E 96-95 (11) procedure. Water vapor permeation was evaluated to determine levels of moisture (sweat) that the membranes can transport providing cooling effect to the wearer. And dimethylmethylphosphonate (DMMP) transport was evaluated in order to determine the level of protection from chemical agents the membrane will provide. DMMP is a relatively harmless molecule that is often used as a simulant for Sarin agent due to similarities in their structures and physical properties. In our experiments (12), an oven, with nitrogen gas purge passed through a desiccant trap, was stabilized at 35 °C and 10% relative humidity (RH). Vials (20 mL) were filled with 10–15 mL of liquid permeant (water or DMMP) and placed in oven to equilibrate for about 24 hr. At this time, the vials were removed and regular caps were replaced with membrane-lined caps shown in figure 3. These caps with open-top caps and Teflon-lined septa have a 14-mm hole cut in the center of the septa to match the hole in the cap. The membranes were cut into circles with a 22-mm diameter (their thickness measured and recorded with a digital micrometer) and placed inside the cap with the cored septa placed behind to provide air-tight seal. The complete total assembly was weighed and placed back into the oven to initiate the experiments. Changes in vials weights were recorded approximately every 24 hr until sufficient number of data points were collected to make an accurate determination of permeation rates.

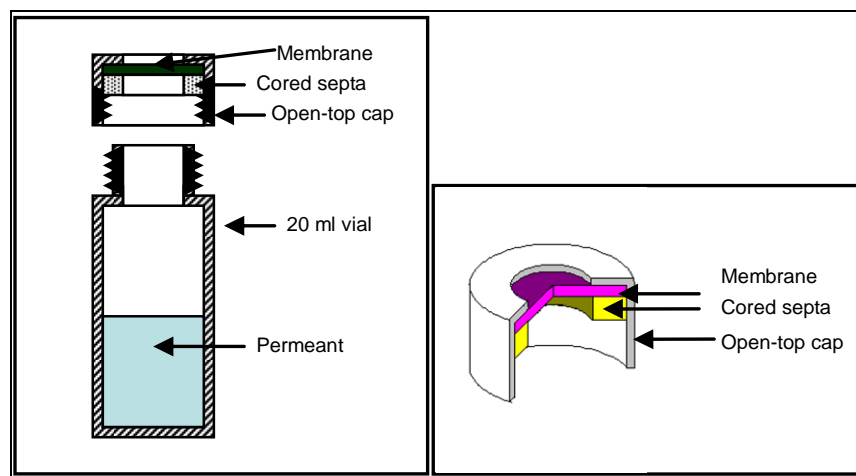


Figure 3. Schematic showing cutaways of the vial-cap and the cap-membrane assemblies used for VTR data collection.

3.5 Thermogravimetric Analysis

Thermogravimetric analysis was performed on a Hi Res TGA 2950 Thermogravimetric Analyzer. Analyses were performed under nitrogen gas purge with temperature ramp from 35 to 700 °C at rate of 10 °C/min using ceramic baskets. Materials specimens weighed between 5 and 15 mg, as recommended by the instrument manufacturer.

4. Results and Discussion

4.1 Levels of Mg Exchange

Levels of magnesium in the exchanged membranes were determined by elemental analysis (EA). This was accomplished by using the relative measured amounts of sulfur and magnesium in the polymer, and calculating percent of sulfur atoms complexed with cation using assumption that each magnesium ion will be ionically attracted to two adjacent sulfuric acid groups. Thus, maximum loading is one magnesium ion per two sulfuric groups. The Mg^{+2} exchange level, shown in table 1, is defined here as percent of complete substitution of acidic hydrogens on the sulfonate ligands with magnesium ions. So, 100% exchange level would signify that all SO_3 groups are ionically bonded to magnesium, 50% exchange level would signify that 50% of all sulfuric groups are bonded to magnesium, etc.

Table 1. Ion exchange levels and elemental analysis results.

| Sample | Equivalents Mg Ions in Solution | Mg to S Ratio Based on EA | Exchange Level Based on EA |
|-------------|---------------------------------|---------------------------|----------------------------|
| Mg-SIBS-Max | 50 | 0.510 | 100 |
| Mg-SIBS-100 | 1 | 0.310 | 62 |
| Mg-SIBS-75 | 0.75 | 0.250 | 50 |
| Mg-SIBS-50 | 0.5 | 0.160 | 32 |
| Mg-SIBS-25 | 0.25 | 0.090 | 18 |
| Mg-SIBS-7 | 0.076 | 0.040 | 8 |
| Mg-SIBS-4 | 0.038 | — | — |
| Mg-SIBS-2 | 0.019 | — | — |
| Mg-SIBS-1 | 0.0076 | — | — |
| Mg-SIBS-0.4 | 0.004 | — | — |
| Mg-SIBS-0 | 0 | — | — |

Examining the relationship between amount of Mg^{+2} ions available for exchange and amount successfully complexed with sulfonate groups (figure 4), we find exchange efficiency factor of 0.641 (obtained from slope of linear regression of the data). Since it remains constant over a long range, we can use this efficiency factor to estimate Mg^{+2} levels in samples that were not evaluated by EA (shown in table 2). Those values are probably not very exact, but they still will be able to provide us with a general idea of what trends occur at very low levels of ion exchange levels.

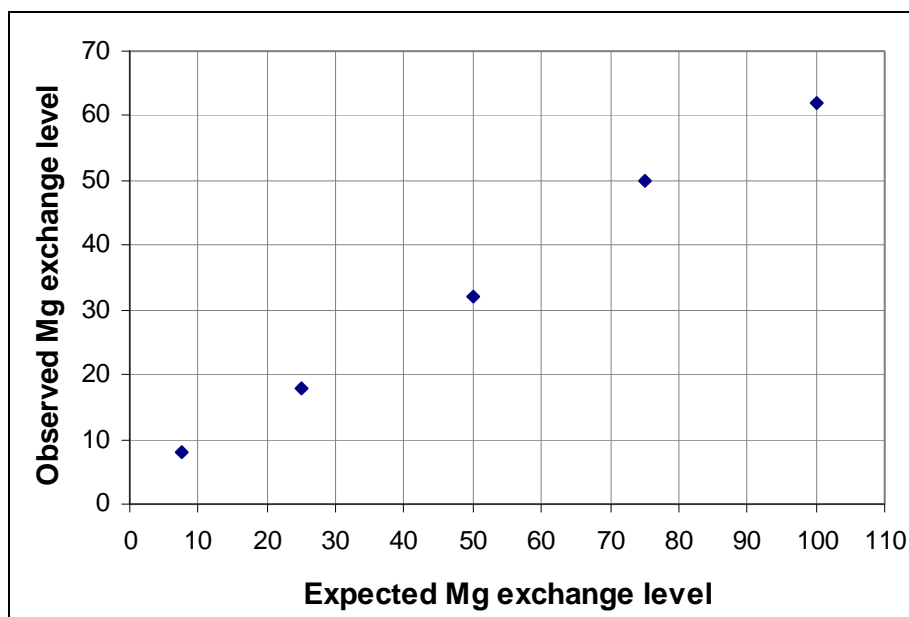


Figure 4. Efficiency of Mg^{+2} - SO_3 complexation reaction.

Table 2. Estimated magnesium levels for low exchange level samples.

| Sample | Equivalents Mg Ions in Solution | Possible Exchange Level | Estimated Exchange Level |
|-------------|---------------------------------|-------------------------|--------------------------|
| Mg-SIBS-4 | 0.038 | 3.8 | 2.4 |
| Mg-SIBS-2 | 0.019 | 1.9 | 1.2 |
| Mg-SIBS-1 | 0.0076 | 0.76 | 0.5 |
| Mg-SIBS-0.4 | 0.004 | 0.4 | 0.3 |
| Mg-SIBS-0 | 0 | 0 | 0 |

4.2 FTIR

Figure 5 shows the infrared spectra of sulfonated and unsulfonated SIBS. There are a number of vibrational stretching bands that appear between 1000 and 1200 cm^{-1} in the sulfonated polymers that do not appear in the unsulfonated polymer. In particular, three distinct bands associated with sulfonic acid were identified in the sulfonated polymers at 1125 , 1034 , and 1007 cm^{-1} . The 1007 and 1125 cm^{-1} vibrational stretching bands represent the in-plane bending vibration of the aromatic ring substituted with the sulfonate group in the para-position and the sulfonated anion attached to the aromatic ring, respectively. The band at 1034 cm^{-1} represents the symmetric and asymmetric stretching vibration of the sulfonate group, respectively. The intensity of this band can be an accurate measure of the amount of sulfonation (4).

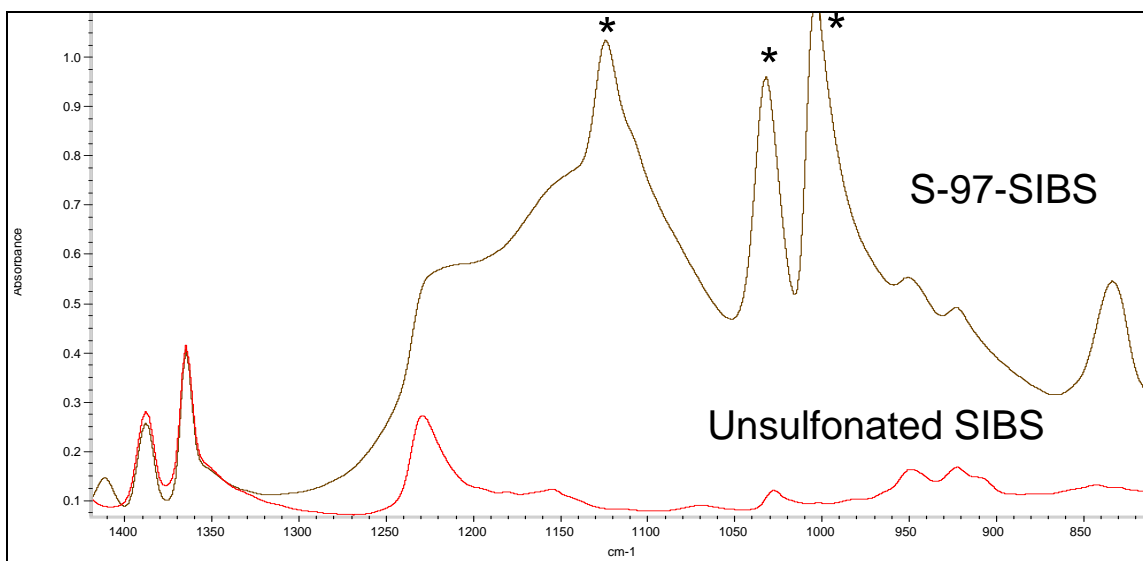


Figure 5. FTIR comparison of sulfonated (S-97-SIBS) and unsulfonated SIBS membranes. Asterisks mark the IR bands associated with sulfonate groups.

It is of interest to compare the IR spectra of the unneutralized and partially neutralized SIBS ionomers. Figure 6 shows the comparison of the acid form SIBS and five Mg^{+2} neutralized SIBS membranes. Generally, little spectral differences are observed for the unneutralized membrane when compared to the 18 % and 32% neutralized membranes. However, above 32% neutralization a new spectral feature appears. An increase in the 1168 cm^{-1} band is observed. This band increases with increasing Mg^{+2} levels. Figure 7 presents the intensity of the 1168 cm^{-1} band as a function of mole % Mg exchanged. This suggests the formation of an Mg-sulfonate complex. The fact that this not seen in the IR spectra at lower Mg^{+2} levels suggests that a concentration percolation threshold occurs with respect to the concentration of the complex. Essentially, if there a 1:1 ratio exists between Mg^{+2} and sulfonate, then no complex is formed. However, as the concentration of Mg is increased and incorporated into the ionic domains, the Mg has the capability to complex to two sulfonate groups, thus creating a 1:2 (Mg:S) ratio, which gives rise to the 1168 cm^{-1} band. Previous research by Belfiore et al. (13) and more recently by Zhu et al. (14) have pointed out that a shift to higher frequency occur in the IR spectra when Co is complexed with SO_3 groups. Figure 7 presents the intensity of the 1168 cm^{-1} band as a function of mole % Mg^{+2} exchanged, which shows this effect more clearly.

Another interesting observation in the FTIR spectra is how the IR bands at 1125 , 1034 , and 1007 cm^{-1} sharpen upon incorporation of Mg^{+2} . As previously discussed, each of these bands are directly related to various stretching modes of the sulfonate groups. This trend is usually observed when an increase in structural ordering is occurring within the polymer matrix. It is plausible to conclude that the incorporation of the Mg^{+2} ions form a highly ordered ionic domains.

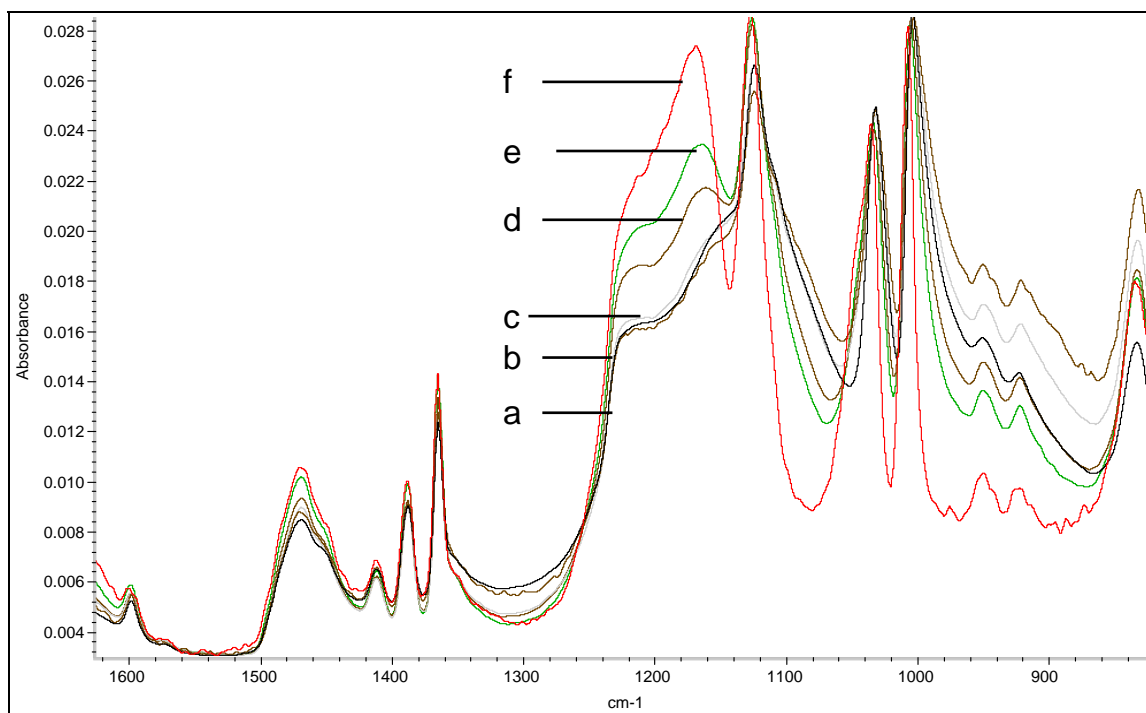


Figure 6. FTIR spectra for neutralized and partially neutralized and non-neutralized SIBS-Mg ionomer, (a) Mg-SIBS-0, (b) Mg-SIBS-25, (c) Mg-SIBS-50, (d) Mg-SIBS-75, (e) Mg-SIBS-100, and (f) Mg-SIBS-Max.

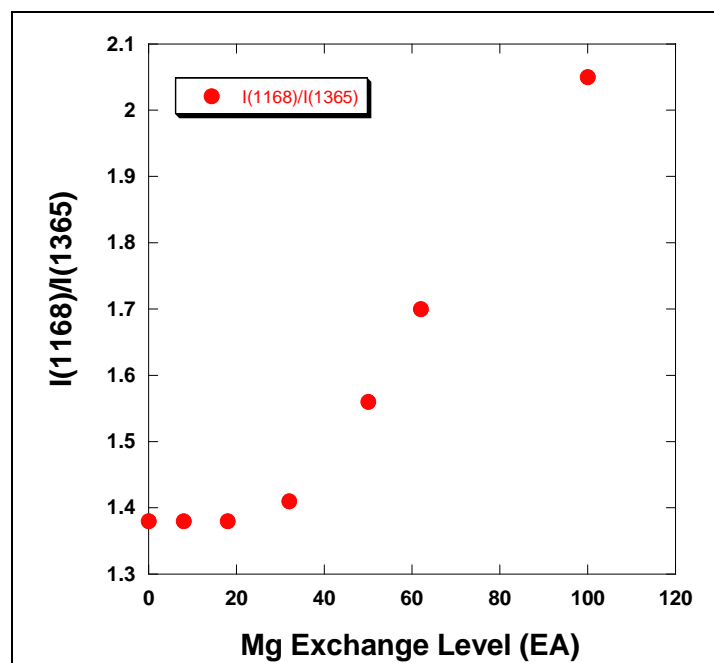


Figure 7. Normalized IR intensity of the 1168 cm^{-1} absorption band with increasing Mg content. This band indicates Mg complexation formed when two or more sulfonate groups ionically bonded to the Mg^{+2} cation.

4.3 Solubility

Water absorption capacity was obtained by swelling polymers in deionized water for 48 hr at room temperature and examining change in sample weights, it is defined here as:

$$\text{wt}\% = \frac{(\text{wet polymer wt} - \text{dry polymer wt})}{\text{dry polymer wt}} \times 100 . \quad (1)$$

The complete data set collected for the all samples can be found in appendix A.

Water absorption capacity of magnesium exchanged S-97-SIBS membranes shows a linear correlation to levels of exchange (figure 8). It varies from 410 weight-percent increase for the non-ion-modified (Mg-SIBS-0) membrane to a 118 weight-percent for the fully exchanged membrane Mg-SIBS-Max. Overall, there is a good correlation between the level of magnesium cations in the membrane and the water mass uptake with very low scatter.

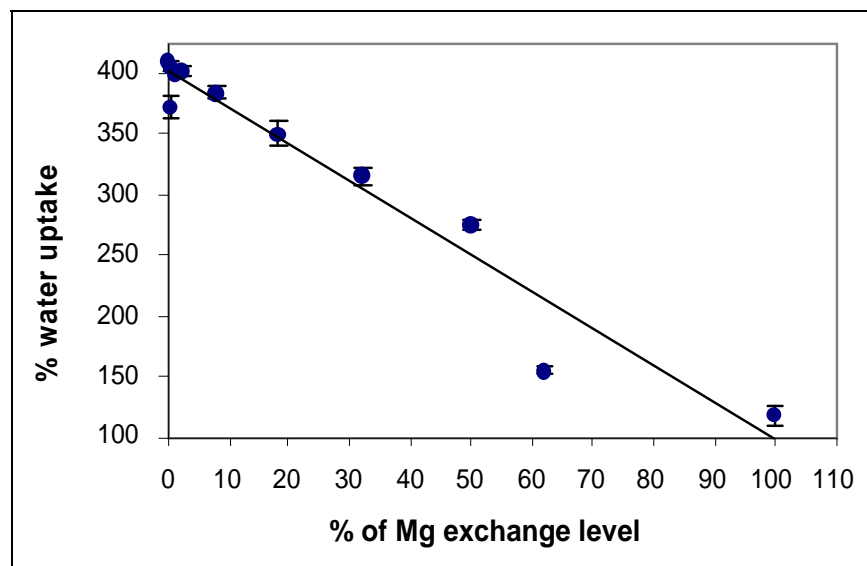


Figure 8. Correlation between water sorption and Mg exchange level.

The only significant deviation to this pattern is Mg-SIBS-100 membrane. The water sorption value for that sample is significantly lower than one would expect. The reason for this is unknown.

4.4 Vapor Transport Rate

Individual vials containing permeant were covered with the experimental membranes and places in to the oven with nitrogen purge. As the weight decreased, it was plotted against time and the slopes of individual curves were determined. The vapor transport rate (VTR) was calculated as:

$$VTR = slope / A , \quad (2)$$

where *slope* is the slope of the resultant straight line (expressed in g/day) and *A* is the area of the polymer film exposed to permeant vapor and is equal to $1.539 \times 10^{-4} \text{ m}^2$ which corresponds to the area of the 14-mm-diameter circle.

Figure 9 shows the water and DMMP vapor transport rates plotted against Mg^{+2} levels. As one would expect, both permeants show a similar trend; a significant decrease in VTR when the Mg^{+2} concentration is elevated. The membrane with the highest levels of the ions, Mg-SIBS-Max (Mg^{+2} exchange level of 100%) provides highest resistance to DMMP vapor. The membranes with the lowest Mg loading produce highest water vapor transport, but also have the lowest resistance to the DMMP vapor. Significant variations in VTR values are observed at low Mg^{+2} concentrations, this is likely due non-homogenous complexation of cation to sulfonic groups and possibly random disruptions to lamellar morphology.

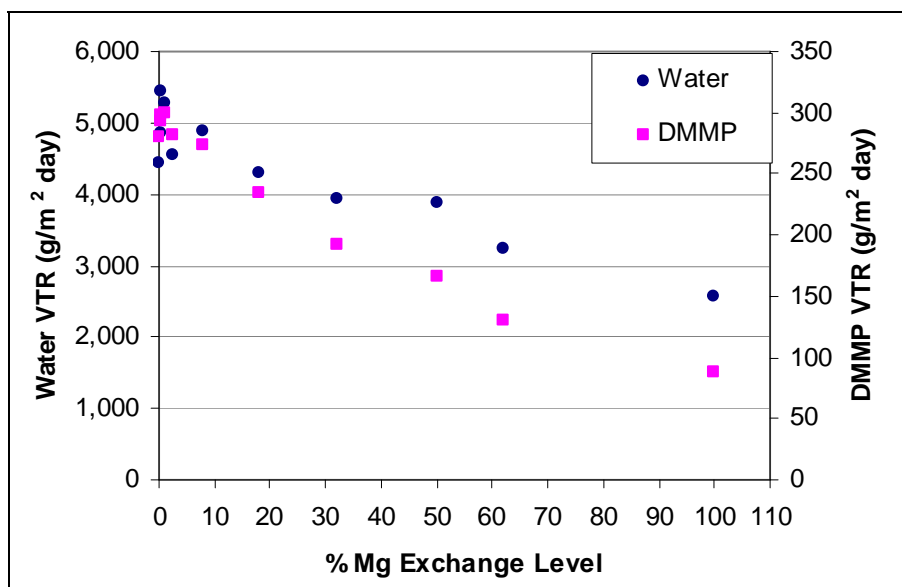


Figure 9. Effect of Mg^{+2} loading on water and DMMP vapor transport.

Selectivity is a useful guide for comparing effectiveness of materials for selective transport of different entities. It does not account for the absolute flux values for each of the permeants, but it does provides a numerical value comparing relative permeabilities of different molecules through the membrane. It is calculated by taking ratio of effective permeability (P_{eff}) of water and effective permeability of DMMP. Effective permeability is defined as:

$$P_{\text{eff}} = \frac{L * VTR}{S * (P_1 - P_2)} , \quad (3)$$

where S is the saturation vapor pressure at the test temperature (mmHg), P_1 is the partial pressure or relative humidity on the challenge side, P_2 is partial pressure on the exit side, and L is the sample thickness (m). Numerical values calculated for all the samples can be found in appendix A.

The selectivity as a function of Mg^{+2} ion loading is shown in figure 10. In general, the selectivity does not change all that much for the 0%–8% portion of the curve. However, a significant increase in the selectivity is observed in the 18%–100% region of the curve. It is interesting that this portion of the curve behaves in this fashion in that it appears to be similar to the observations in the FTIR spectra in figure 6. Our previous results in the FTIR section concluded that a complex is formed when the Mg^{+2} level reaches 32% exchange level. It begins to become apparent that the transport behavior is demonstrating the same behavior, where the percolation is also around 32% neutralized.

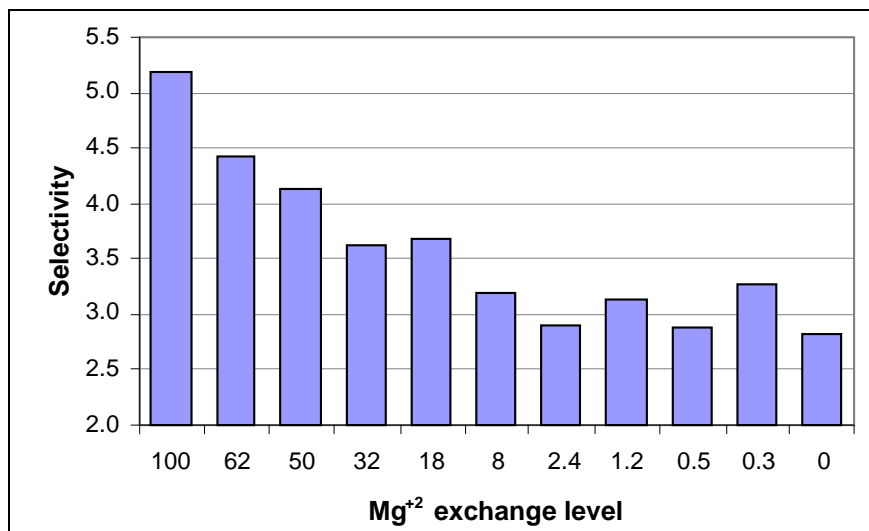


Figure 10. Water-DMMP selectivity of Mg^{+2} exchanged SIBS.

A different way to view this trend is to plot the VTR for both DMMP and water against each other. Figure 11 show that this change occurs around the 18% exchange level. Until that level, incorporation of Mg^{+2} cations into sulfonated SIBS membrane effects primarily water transport and have very limited effect on the DMMP VTR. At level of exchange 18% and above, resistance to DMMP begins to improve dramatically. This figure also provides us with information on another interesting property of partially exchanged membranes. Since different Mg^{+2} loadings affect the absolute permeation rate of the vapors over a very wide range, it would be possible to design a membrane that will transport vapors of interest at a specific and controlled rate by selecting appropriate levels of the cation.

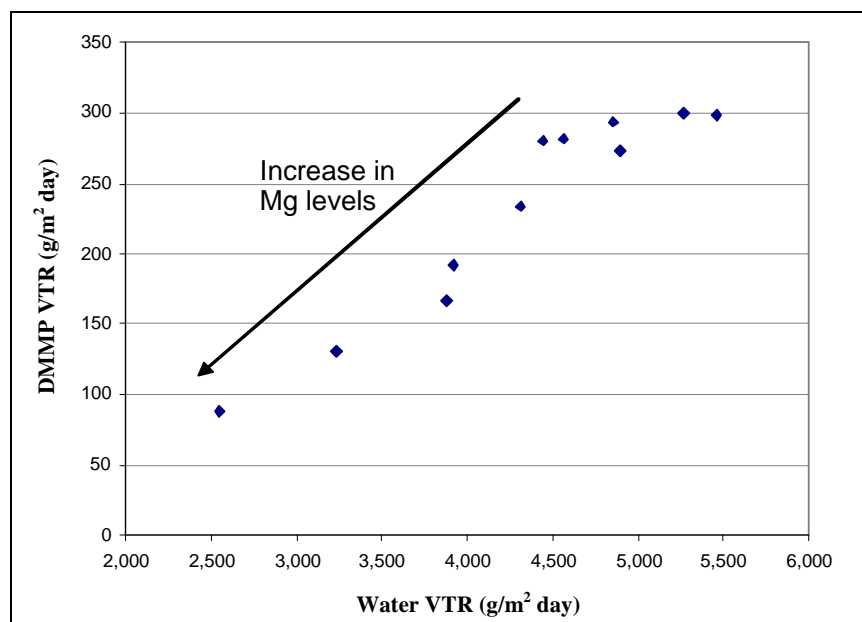


Figure 11. Correlation between water and DMMP vapor transport rates.

4.5 TGA

Ionically exchanged SIBS and similar materials have been evaluated via thermogravimetric analysis (TGA) in the past (15, 16). It was shown that the incorporation of cations significantly improves the thermal stability of sulfonic groups by shifting their initial decomposition temperatures from 200 to 300 °C to about 550 °C. Thus, the overall stability of polymer is increased from 200 to 300 °C (where sulfonic acid groups thermally decompose) to ~400 °C, at which point isobutylene and polystyrene backbone decomposes.

Varying Mg^{+2} ion content also has some interesting effects on thermal properties of these samples (complete numerical results obtained from all TGA experiments can be found in appendix B) that were observed during evaluation of derivative of weight loss curves (DTGA). Observing the position of the onset of the SO_3 degradation peak (17) at 200–300 °C, it is plainly visible how the peak onset is changing with increasing Mg^{+2} ion content (see figure 12a). Plotting the degradation onset temperature vs. level of magnesium exchange (shown in figure 12b) makes these observations even more compelling. Again, like in the experiments involving vapor permeation, this polymer behavior changes significantly at 18% ion exchange level. Thermal stability of sulfonate/ Mg^{+2} complexes decreases by as much as 24 °C as compared to acid form of the polymer, and not until 18% exchange level is obtained do we show improvement in thermal stability. At which point the peak onset temperature begins to increase linearly with the ion exchange levels.

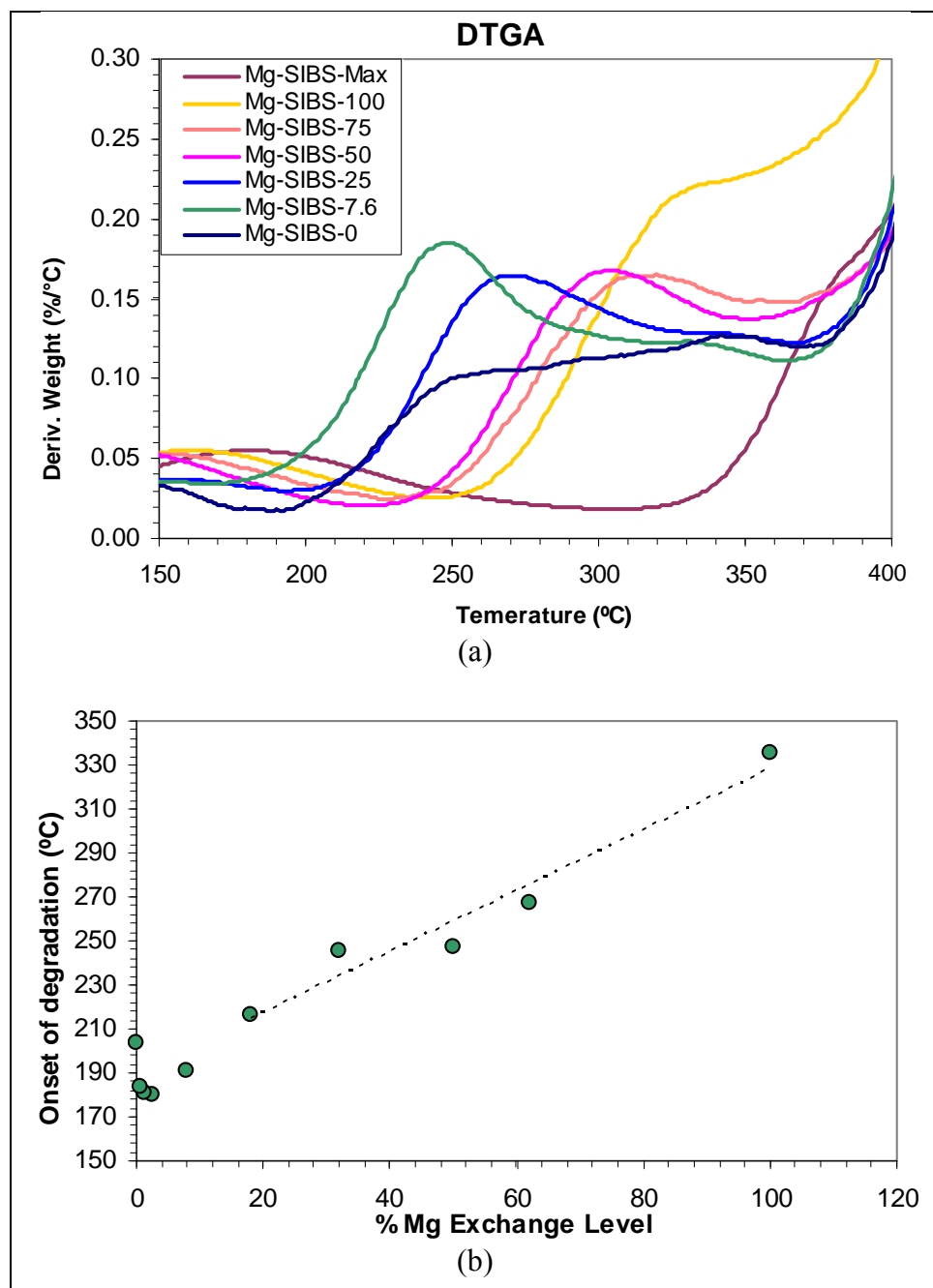


Figure 12. Visual representation of shift in SO_3 decomposition temperature, (a) as an overlay of DTGA curves and (b) as a plot of the onset temperature vs. % Mg^{+2} exchange levels.

Another feature obtained from the TGA experiments that can be evaluated is decomposition of what is believed to be Mg-SO₃ complex observed in the 550–600 °C region of the DTGA curves (figure 13a). An increased weight loss in this region can be attributed to the increasing amounts of ionically crosslinked sulfonic groups (16). The area under the DTGA decomposition peaks was normalized to initial sample weight and plotted vs. magnesium exchange levels (figure 13b), which resulted in a poor correlation. The issue is complicated by presence of multiple peaks, present in some and absent in other formulations. It is possible that this is caused by existence of different types of Mg-SO₃ complexes but it needs to be investigated further. Interestingly, for samples below 18% of ion exchange we still observe the same counterintuitive behavior that was seen in evaluation of the 200 °C weight loss onset. If nothing else, this data can be used as an indicator that those strange temperature shifts are indeed real, and not a random instrumental scatter.

5. Conclusions

In this study, the vapor transmission rate and effective permeability of water and DMMP (a stimulant for the nerve agent Sarin) were measured for a series of ionic polymer membranes that have been partially neutralized with Mg counterions. In addition, the FTIR spectra and TGA were performed to determine both the structure of the ionic polymer as well as the overall thermal stability. It was determined that partial exchange of acidic hydrogen in sulfonated SIBS with magnesium ions showed a significant increase in the overall selectivity of the membrane but only when the Mg⁺² levels reached concentration levels above 18%. Selectivity continues to improve until maximum level of cation exchange is reached.

The FTIR results demonstrated convincingly that a complex forms between the Mg⁺² counterion and the sulfonic acid groups of the membrane. This resulted in a membrane that exhibited a considerable amount of structural ordering when compared to the membranes measured without the counterions. The complex and subsequent ordering was only observed when Mg⁺² concentrations reached 50% or greater.

The TGA results showed that changing level of the Mg⁺² counterion crosslinking greatly affects the onset of thermal stability of the membranes. Slightly decreasing decomposition temperature at low levels of exchange (under 18%), and substantially increasing it at higher levels of exchange.

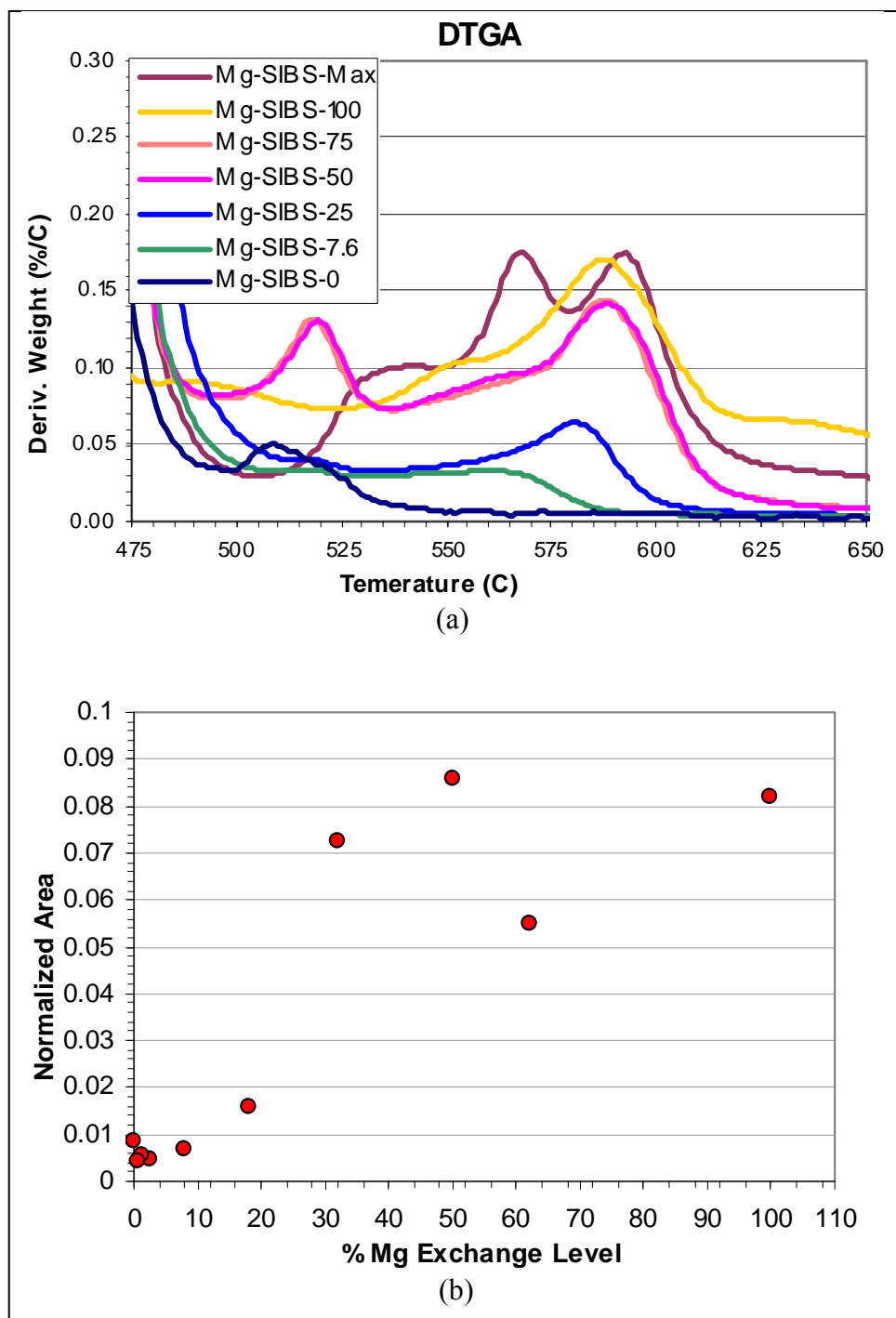


Figure 13. Increase in area under $\text{SO}_3\text{-Mg}$ complex decomposition curves, (a) as an overlay of DTGA curves and (b) as a plot of the area vs. % Mg^{+2} exchange levels.

6. References

1. Lee, B. T.; Yang, T. W.; Wilusz, E. Moisture Effects on Isobutylene-Isoprene Copolymer-Based Composite Barrier. 1. Moisture Diffusion and Detection. *Polym. Eng. Sci.* **1996**, *36* (9), 1217.
2. Siegrist, D. Chemical – Biological Warfare: Protective Measures. *Jane's Defence Weekly* 17 April **2002**.
3. Elabd, Y. A.; Napadensky, E.; Sloan, J. M.; Crawford D. M.; Walker, C. W. Triblock Copolymer Ionomers Membranes. Part I. Methanol and Proton Transport. *J. Membr. Sci.* **2003**, *217*, 227–242.
4. Elabd, Y. A.; Napadensky, E. Sulfonation and Characterization of Poly(styrene-isobutylene-styrene) Triblock Copolymers at High Ion-Exchange Capacities. *Polymer* **2004**, *45*, 3037.
5. Lu, X.; Steckle, W. P.; Weiss, R. A. Ionic Aggregation in a Block Copolymer Ionomer. *Macromolecules* **1993**, *26*, 5876.
6. Hamley, I. W. *The Physics of Block Copolymers*; Oxford University Press: New York, NY, 1998.
7. Elabd, Y. A.; Napadensky, E.; Walker, C. W.; Winey, K. I. Transport Properties of Sulfonated Poly(styrene-b-isobutylene-b-styrene) Triblock Copolymers at High Ion-Exchange Capacities. *Macromolecules* **2006**, *39*, 399–407.
8. Schneider, N. S.; Rivin, D. Interaction of Dimethyl Methylphosphonate with Nafion in Acid and Cation Modifications. *Polymer* **2004**, *45*, 6309–6320.
9. Weiss, R. A.; Sen, A.; Pottick, L. A.; Willis, C. L. Block Copolymers Ionomers 2: Viscoelastic and Mechanical Properties of Sulfonated Poly(Styrene-Ethylene-Butylene Styrene). *Polymer* **1991**, *32*, 2785.
10. Weiss, R. A.; Sen, A.; Willis, C. L.; Pottick, L. A. Block Copolymers Ionomers 1: Synthesis and Physical Properties of Sulfonated Poly(Styrene-Ethylene-Butylene Styrene). *Polymer* **1991**, *32*, 1867.
11. ASTM E 96-95. Standard Test Methods for Vapor Transmission of Materials. American Society for Testing & Materials. *Annu. Book ASTM Stand.* **2002**.
12. Elabd, Y. A.; Napadensky, E. *Breathability and Selectivity of Selected Materials for Protective Clothing*; ARL-TR-3235; U.S. Army Research Laboratory: Aberdeen Proving Ground, MD, 2004.

13. Belfiore, L. A.; Pires, A. T. N.; Wang, Y.; Graham, H.; Ueda, E. Transition Metal Coordination in Polymer Blends and Model Systems. *Macromolecules* **1992**, 25 (5), 1411.
14. Zhu, R.; Wang, Y.; He, W. Multiple Morphological Micelles Formed From the Self-Assembly of Poly(styrene-*b*-poly(4-vinylpyridine) Containing Cobalt Dodecyl Benzene Sulfonate. *Eur. Polym. J.* **2005**, 41, 2088.
15. Suleiman, D.; Elabd, Y. A.; Sloan, J. M.; Napadensky, E.; Crawford, D. M. Thermogravimetric Characterization of Highly Sulfonated Poly (Styrene-Isobutylene-Styrene) Block Copolymers: Effects of Processing Conditions. *Thermochim. Acta* **2005**, 430, 149.
16. Suleiman, D.; Sloan, J. M.; Napadensky, E.; Crawford, D. M. Thermogravimetric Characterization of Highly Sulfonated Poly (Styrene-Isobutylene-Styrene) Block Copolymers: Effects of Sulfonation and Counterion Substitution. *Thermochim. Acta* **2007**, 460, 35.
17. Jiang, D. D.; Yao, Q.; McKinney, M. A.; Wilkie, C. A. TGA/FTIR Studies on the Thermal Degradation of Some Polymeric Sulfonic and Phosphonic Acids and their Sodium Salts. *Polym. Degrad. Stab.* **1999**, 63, 423–434.

INTENTIONALLY LEFT BLANK.

Appendix A. Solubility and Transport Data

Table A-1. Water sorption data.

| Sample | Theoretical % Exchange | Actual % Exchange | Average Weight Dry (mg) | Average Weight Wet (mg) | % H ₂ O Uptake |
|-------------|------------------------|-------------------|-------------------------|-------------------------|---------------------------|
| Mg-SIBS-Max | Max | 100 | 19.5 | 42.6 | 118.5 |
| Mg-SIBS-100 | 100 | 62 | 16 | 40.9 | 155.4 |
| Mg-SIBS-75 | 75 | 50 | 17.2 | 64.5 | 275.0 |
| Mg-SIBS-50 | 50 | 32 | 9.9 | 41.1 | 315.2 |
| Mg-SIBS-25 | 25 | 18 | 9.7 | 43.7 | 350.2 |
| Mg-SIBS-7 | 7.6 | 8 | 22.2 | 107.5 | 384.4 |
| Mg-SIBS-4 | 3.8 | 2.4 | 15.1 | 75.8 | 401.8 |
| Mg-SIBS-2 | 1.9 | 1.2 | 25.8 | 128.9 | 399.5 |
| Mg-SIBS-1 | 0.76 | 0.5 | 10.3 | 52.2 | 406.3 |
| Mg-SIBS-0.4 | 0.4 | 0.3 | 16.5 | 78.0 | 372.9 |
| Mg-SIBS-0 | 0 | 0 | 13.1 | 66.8 | 409.9 |

Table A-2. Vapor transport data.

| Sample | Water VTR g/m ² Day | | Water Effective Perm. (g/mmHg m Day) | | DMMP VTR g/m ² Day | | DMMP Effective Perm. (g/mmHg m Day) | | Selectivity |
|-------------|-----------------------------------|-------|---|--------|----------------------------------|-------|--|--------|-------------|
| | AVG | STDEV | AVG | STDEV | AVG | STDEV | AVG | STDEV | |
| Mg-SIBS-Max | 2554 | 83 | 0.0072 | 0.0009 | 88 | 9 | 0.0014 | 0.0001 | 5.2 |
| Mg-SIBS-100 | 3236 | 328 | 0.0088 | 0.0013 | 130 | 21 | 0.0020 | 0.0004 | 4.4 |
| Mg-SIBS-75 | 3879 | 221 | 0.0084 | 0.0010 | 167 | 8 | 0.0020 | 0.0003 | 4.1 |
| Mg-SIBS-50 | 3922 | 80 | 0.0118 | 0.0060 | 192 | 21 | 0.0033 | 0.0011 | 3.6 |
| Mg-SIBS-25 | 4307 | 188 | 0.0106 | 0.0011 | 234 | 17 | 0.0029 | 0.0001 | 3.7 |
| Mg-SIBS-7 | 4890 | 220 | 0.0111 | 0.0005 | 273 | 5 | 0.0035 | 0.0002 | 3.2 |
| Mg-SIBS-4 | 4559 | 343 | 0.0136 | 0.0024 | 282 | 15 | 0.0047 | 0.0011 | 2.9 |
| Mg-SIBS-2 | 5270 | 376 | 0.0107 | 0.0008 | 300 | 26 | 0.0034 | 0.0004 | 3.1 |
| Mg-SIBS-1 | 4850 | 110 | 0.0117 | 0.0001 | 294 | 15 | 0.0041 | 0.0002 | 2.9 |
| Mg-SIBS-0.4 | 5452 | 116 | 0.0151 | 0.0009 | 298 | 5 | 0.0046 | 0.0002 | 3.3 |
| Mg-SIBS-0 | 4437 | 189 | 0.0127 | 0.0017 | 280 | 7 | 0.0045 | 0.0008 | 2.8 |

Appendix B. TGA Data

Table B-1. TGA data.

| Sample | SO₃ Degradation Peak (°C) | Peak Area at 500–600 °C | Sample Weight (mg) | Normalized Area (Area/Weight) |
|---------------|---|------------------------------------|-----------------------------------|--|
| Mg-SIBS-Max | 335 | 0.7591 | 93278 | 0.0818 |
| Mg-SIBS-100 | 267 | 0.3941 | 7.152 | 0.0551 |
| Mg-SIBS-75 | 247 | 0.4894 | 5.702 | 0.0858 |
| Mg-SIBS-50 | 245 | 0.5241 | 7.212 | 0.0727 |
| Mg-SIBS-25 | 216 | 0.1306 | 8.133 | 0.0161 |
| Mg-SIBS-7 | 191 | 0.0660 | 9.322 | 0.0071 |
| Mg-SIBS-4 | 180 | 0.0344 | 7.4625 | 0.0046 |
| Mg-SIBS-2 | 180.5 | 0.0396 | 7.2295 | 0.0055 |
| Mg-SIBS-1 | 183.5 | 0.0344 | 7.7815 | 0.0044 |
| Mg-SIBS-0 | 204 | 0.0442 | 5.037 | 0.0088 |

NO. OF
COPIES ORGANIZATION

1 DEFENSE TECHNICAL
(PDF INFORMATION CTR
only) DTIC OCA
8725 JOHN J KINGMAN RD
STE 0944
FORT BELVOIR VA 22060-6218

1 US ARMY RSRCH DEV &
ENGRG CMD
SYSTEMS OF SYSTEMS
INTEGRATION
AMSRD SS T
6000 6TH ST STE 100
FORT BELVOIR VA 22060-5608

1 DIRECTOR
US ARMY RESEARCH LAB
IMNE ALC IMS
2800 POWDER MILL RD
ADELPHI MD 20783-1197

1 DIRECTOR
US ARMY RESEARCH LAB
AMSRD ARL CI OK TL
2800 POWDER MILL RD
ADELPHI MD 20783-1197

1 DIRECTOR
US ARMY RESEARCH LAB
AMSRD ARL CI OK T
2800 POWDER MILL RD
ADELPHI MD 20783-1197

ABERDEEN PROVING GROUND

1 DIR USARL
AMSRD ARL CI OK TP (BLDG 4600)

NO. OF
COPIES ORGANIZATION

ABERDEEN PROVING GROUND

17 DIR USARL
AMSRD ARL WM M
S MCKNIGHT
AMSRD ARL WM MA
J ANDZELM
D CRAWFORD
L GHORSE
E NAPADENSKY (10 CPS)
A RAWLETT
J SLOAN
M VANLANDINGHAM